JACS
JOURNAL OF THE AMERICAN CHEMICAL SOCIETY
Article
pubs.acs.org/JACS

Mechanism of Formation of Supramolecular DNA-Templated Polymer Nanowires

Scott M. D. Watson, Miguel A. Galindo, Benjamin R. Horrocks, and Andrew Houlton*

Chemical Nanoscience Laboratories, School of Chemistry, Newcastle University, Bedson Building, Newcastle upon Tyne, NE1 7RU United Kingdom

Supporting Information

ABSTRACT: Details of the mechanism of formation of supramolecular polymer nanowires by templating on DNA are revealed for the first time using AFM. Overall these data reveal that the smooth, regular, structures produced are rendered by highly dynamic supramolecular transformations occurring over the micrometre scale. In the initial stages of the process a low density of conducting polymer (CP) binds to the DNA as, essentially, spherical particles. Further reaction time produces DNA strands which are more densely packed with particles giving a beads-on-a-string appearance. The particles subsequently undergo dynamic reconfiguration so as to elongate along the template axis and merge to yield the highly regular, smooth morphology of the final nanowire. MD simulations illustrate the early stages of the process showing the binding of globular CP to duplex DNA, while the latter stages can be modeled effectively by a linear thermodynamic description based on the balance between the line energy, which accounts for adhesion of the material to the template, and its surface tension. This model accounts for the phenomena observed in the AFM studies: the relative success of DNA templating of polymers compared to metals; the slow approach to equilibrium; and the observed thinning and 'necking' phenomena as the structures transform from beads-on-a-string to smooth nanowire.

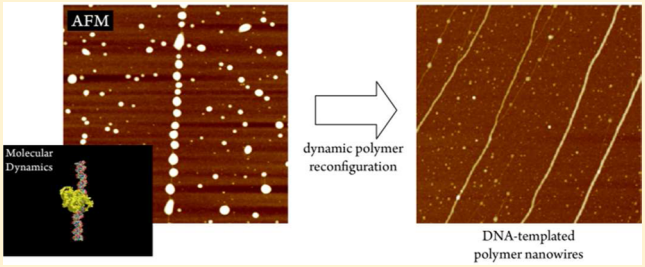

INTRODUCTION

For a variety of reasons, ranging from economics to possibilities for new types of computing architectures, there is great interest in the development of bottom-up routes to the assembly of functional electronics.[1] Such an approach requires the availability of suitable building blocks, e.g., nanowires as interconnects, and means by which to organize these into particular circuit arrangements.[2−4] Wet chemical methods, based on self-assembly, offer simple, economical, and scaleable routes to such systems and, among the various approaches being explored, one based on DNA is emerging as addressing many of the necessary features for the concept.[5−9] The structure building rules of base pairing provide a powerful means by which to design and assemble nanostructured architectures over micrometer length scales. The types of structures produced include 2D lattices,[10] tubes and braids,[11] and 3D polyhedra.[12] With the more recent development of "DNA-origami", an almost limitless ability to design and construct geometrically complex structures has been achieved.[13−16]

While the ability to introduce presynthesized components, such as carbon nanotubes[17] and Au nanoparticles,[18−21] into DNA-based nanostructures has been demonstrated, an alternative method by which to introduce appropriate materials and functionality is offered by templating.[7,22,23] Templating exploits the ability of DNA to bind precursors of conducting materials and direct their growth along the duplex. This method has been shown to be compatible with important material types, such as metals[22−26] and compound semiconductors,[27] and with larger, circuit-like, DNA assemblies.[28−3132−34]

More recently DNA-templating, as a method for forming nanowires, has been extended to molecular-based conductors, such as polyaniline,[35−37] polypyrrole,[38,39] and similar compounds.[40−42] The resulting materials are a type of supramolecular polymer[43−46] as they comprise anionic duplex DNA and cationic, synthetic, conducting polymer (CP) strands assembled by noncovalent interactions.[47−50] This method has been shown to be particularly capable of providing structures at the lower end of the nanometre scale range. These polymer nanowires can be remarkably regular and smooth over micrometer lengths, in marked contrast to many cases of similarly prepared metal-containing systems.[5,51] Critically, they are conductive and can even exhibit enhanced conductivities compared to bulk material.[38,41]

While the number of examples of polymer nanowires formed by DNA-templating has increased significantly, there have been, to our knowledge, no reports that explore the growth mechanism of this type of supramolecular structure. Nanowire formation by this method relies on the complementarity of the CP chains and the DNA duplex. A simplistic view of this process is that the CP, initially formed as short cationic

Received: January 15, 2014
Published: April 8, 2014

   dx.doi.org/10.1021/ja500439v | J. Am. Chem. Soc. 2014, 136, 6649−6655

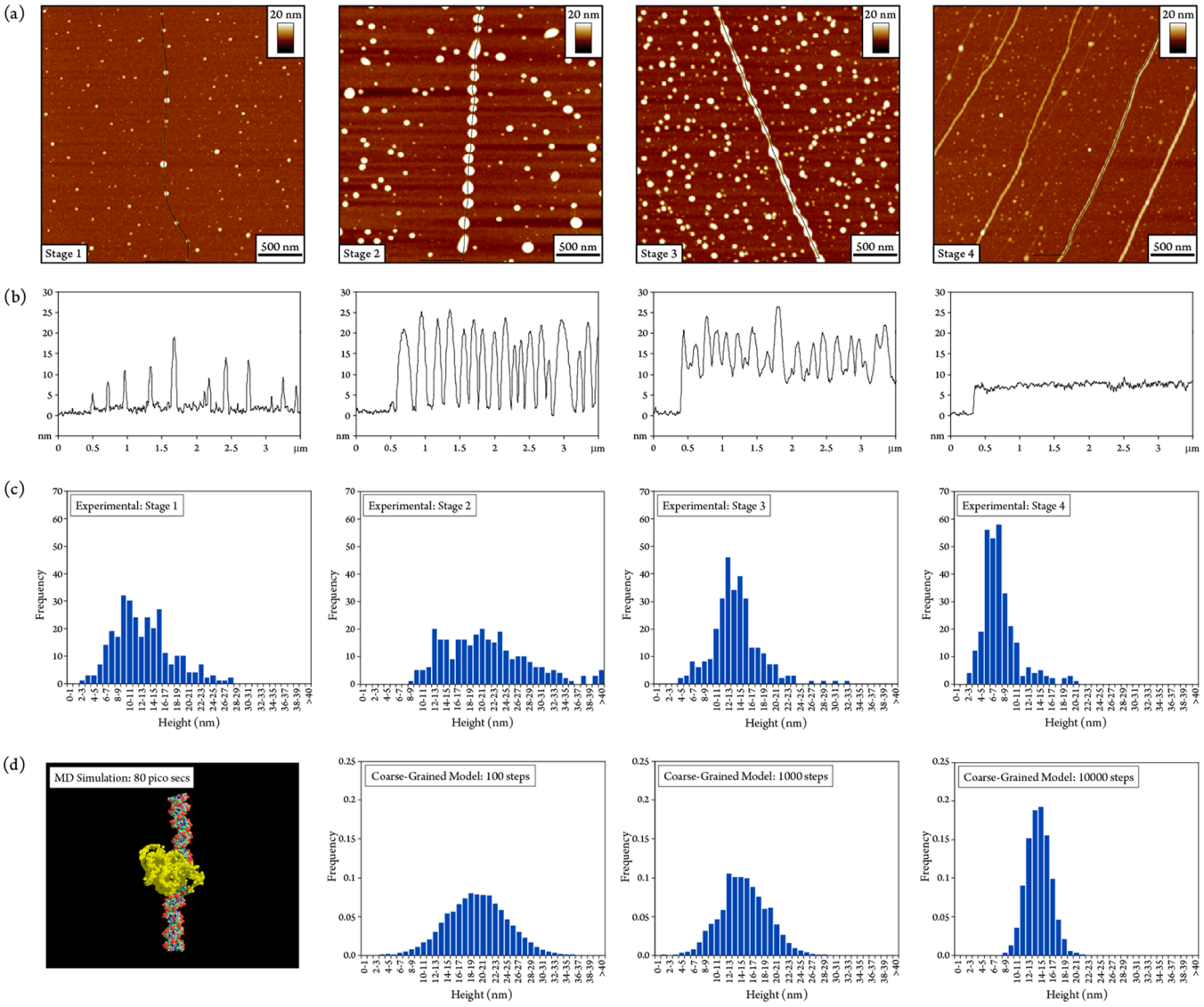

Figure 1. Formation of poly(TPT) nanowires at λ-DNA. (a) Tapping mode AFM images of samples isolated and deposited on TMS-modified Si/SiO_2 substrates identifying four distinct stages in the formation and growth (left to right, Stages 1−4 correspond to ∼10 min and 1, 4, 24 h.) (b) The corresponding line section along the template DNA shown in the images in (a) for each stage. (c) Histograms showing the distribution of nanoparticle or nanowire heights determined from AFM images of 300 particles. (d) Multiscale modeling results. Left to right: MD simulation at 80 ps of nucleation (Stage 1) and histograms from our coarse-grained linear thermodynamics model for the transitions between stages 2, 3, and 4.

oligomers, binds to the DNA through supramolecular interactions, e.g., electrostatics plus additional noncovalent bonding, possibly in a manner analogous to small groove-binding drug molecules.[52] This, then influences the growth of further polymer along the double-helix axis. Here, we provide, for the first time, details of the mechanism of supramolecular nanowire formation by DNA-templating for the representative cases of poly-2,5-bis(2-thienyl)pyrrole (poly(TPT)) and polypyrrole (poly(Py)). Atomic force microscopy (AFM), supported by multiscale modeling, provides insight into the process and reveals a quite different mechanism compared to the simple view. Though clearly continuous, the mechanism may be considered to pass through several, rather structurally distinct, forms and to involve a dramatic reorganization of the CP polymer strands over an exceptionally large, micrometer, length scale once bound to the DNA duplex.

RESULTS AND DISCUSSION

A typical preparation of DNA/CP nanowires involves oxidation of the appropriate monomer in DNA-containing aqueous, or mixed solvent, solution using $FeCl_3$.[38−42] The DNA used was bacteriophage lambda as this provides a long (48,502 bp) and monodisperse template. For reactions with 2,5-bis(2-thienyl)-pyrrole (TPT) the low aqueous solubility of the monomer requires the use of a cosolvent (MeCN), whereas for pyrrole (Py) no cosolvent was needed. Samples were isolated from the reaction mixture at various times and deposited using molecular combing[29] onto trimethylsilane-modified Si/SiO_2 surfaces for subsequent analysis by AFM. (Note: AFM data for control experiments of reactions in the absence of DNA, showing exclusive formation of particulate material, are provided in Figures S1−2).

Formation of Poly(TPT) Nanowires. Figure 1 presents a series of typical AFM TappingMode images for DNA-templating of poly(TPT) at various stages in the reaction;

dx.doi.org/10.1021/ja500439v | J. Am. Chem. Soc. 2014, 136, 6649−6655

Scheme 1. Stages in the Growth Mechanism of Supramolecular DNA-Templated Polymer Nanowires[a]

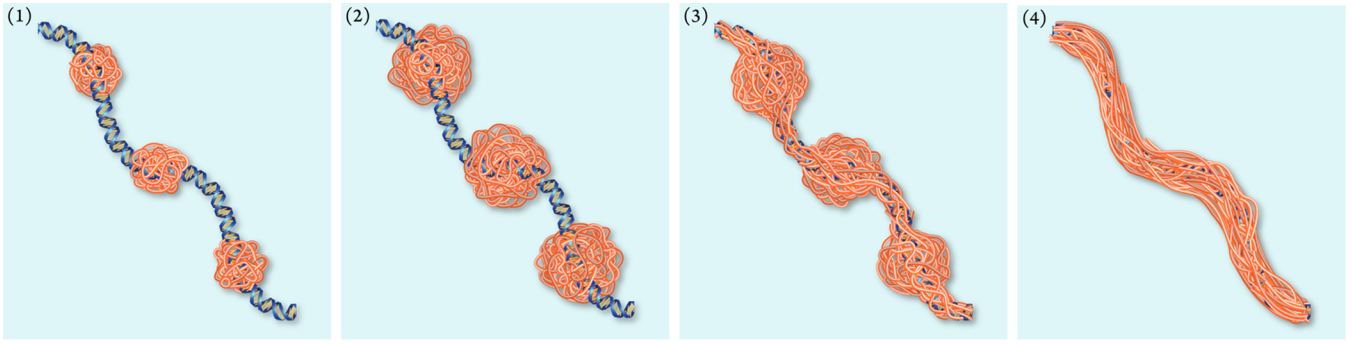

[a](1) Initial polymerization yields a number of small polymer particles which bind to, or nucleate on, the template DNA. (2) The density and size of particles on the template increases producing a "beads-on-a-string" appearance. (3) Transformation of the shape of the DNA-bound polymer particles from spherical to prolate ellipsoids driven by the maximisation of the favorable free energy of adhesion to the template. (4) The final smooth wire-like structure is formed, with diameter markedly smaller than the individual particle sizes at earlier stages.

metrical and statistical data are displayed as well as the results from modeling. In the AFM experiments the heights of the structures were analyzed; in Stages 1 and 2 the histograms show the particle diameters, and in Stages 3 and 4, where the individual particles are not so well-defined, the local maxima in the structure were measured. The evolution of individual nanostructures is not observable, therefore we collected a large number of images and analyzed the distributions of the heights/maxima as histograms. Samples at the early stage of reaction (Stage 1) show evidence of polymer formation and DNA binding. Polymer particles, considered to be globular, are found to be deposited on the substrate as isolated structures as well as bound along individual DNA strands (Figure 1a, column 1 and Figure S3). The DNA molecule here has approximately spherical particles bound at low density with bare DNA clearly evident between adjacent particles. The line section along the single DNA molecule in Figure 1b, column 1, illustrates this showing a density of ∼3 particles/μm as well as the range of particle sizes along this individual strand. Typically, a density of 2−5 poly(TPT) particles per micrometer length of the DNA template was found at this earliest stage. A statistical analysis of 300 DNA-bound particles, shown in the histogram (Figure 1c, column 1), reveals the range of particle sizes to be ∼3−28 nm with a mean of 12.7 nm and a standard deviation of 4.8 nm.

By Stage 2 the density of the particles on the DNA strands has increased, typically 4−7 poly(TPT) particles per micrometer length of the DNA template, however bare regions remain. This can again be appreciated in the AFM height image (Figure 1a, column 2) but also from inspection of the line section drawn along the individual DNA molecule in Figure 1b, column 2, where average density ∼6 particles/μm is now found. The resulting structure can be described as having a dense beads-on-a-string appearance. The size of the DNA-bound particles is also increased, range 10−40 nm (mean = 21.1 nm and standard deviation = 7.2 nm.) (Figure 1c, column 2 and Figure S4). These are still evident as discrete bodies. Close inspection of the image (Figure 1a, column 2) reveals, however, that while the majority of DNA-bound particles retain the, essentially, spherical shape of the earliest stage, some become more prolate, extending in the direction of the template axis.

With further time (Stage 3, Figure 1, column 3) a new morphology appears where the, previously discrete, particles have merged into one another forming an essentially continuous coverage along the template.[53] The line-section traced down the DNA molecule indicated (Figure 1b, column 3) illustrates this, as at no point is the measured height <2 nm; the height corresponding to bare DNA. Even more striking, however, is the pronounced change in morphology and height of the DNA-bound material. Now all the particles have changed shape, becoming extended along the template axis with thinning/necking being evident, as particles merge. It is important to realize that this change in morphology is not significantly as a consequence of additional CP binding to the template. The metrical parameters (Figure 1c, column 2, cf. 3) indicate that this morphological change actually results in a reduction in the size of the DNA-bound material as a result of the dynamic reconfiguration of CP strands on the DNA duplex.

By the final Stage, 4, the morphology of individual strands has transformed into the highly smooth, continuous, uniform structure of the final nanowire (Figure 1a, column 4). Here there is no longer evidence of particle-like features. The absence of significant breaks in the structure is supported by the electrical conductivity along the nanowires.[38,39,41,42] Furthermore, the measured height of these nanowires is markedly reduced compared to the heights of the largest particles on the template at earlier stages of the formation process (Figure 1c). A typical diameter for the final poly(TPT) nanowire is 5−8 nm, compared with heights as large as 40 nm at earlier stages. As stated, this clearly indicates that the new morphology is not a consequence of additional material binding to sections of the template which was deficient of CP, but instead must arise from a dynamic reconfiguration of the DNA-bound CP strands.

Formation of Poly(Py) Nanowires. In order to establish the generality of this behavior we also studied the formation of nanowires of polypyrrole, poly(Py). Representative AFM images are shown in Figure S6. In this case too, essentially the same stages are noted as the reaction proceeds indicating the similarity in the growth mechanism for these structurally related polymers. There are, however, some differences in the details. First, nanowire formation occurs more rapidly for poly(Py) compared to poly(TPT). Also, even structures with a low density of particles bound to DNA show evidence of the elongation of the poly(Py) particles along the template axis. These differences are perhaps explained by the increased hydrophilicity of the former material; hydrophobic effects will make poly(TPT) nuclei slower to uncoil and rearrange along the template. The overall process is depicted in Scheme 1

dx.doi.org/10.1021/ja500439v | J. Am. Chem. Soc. 2014, 136, 6649−6655

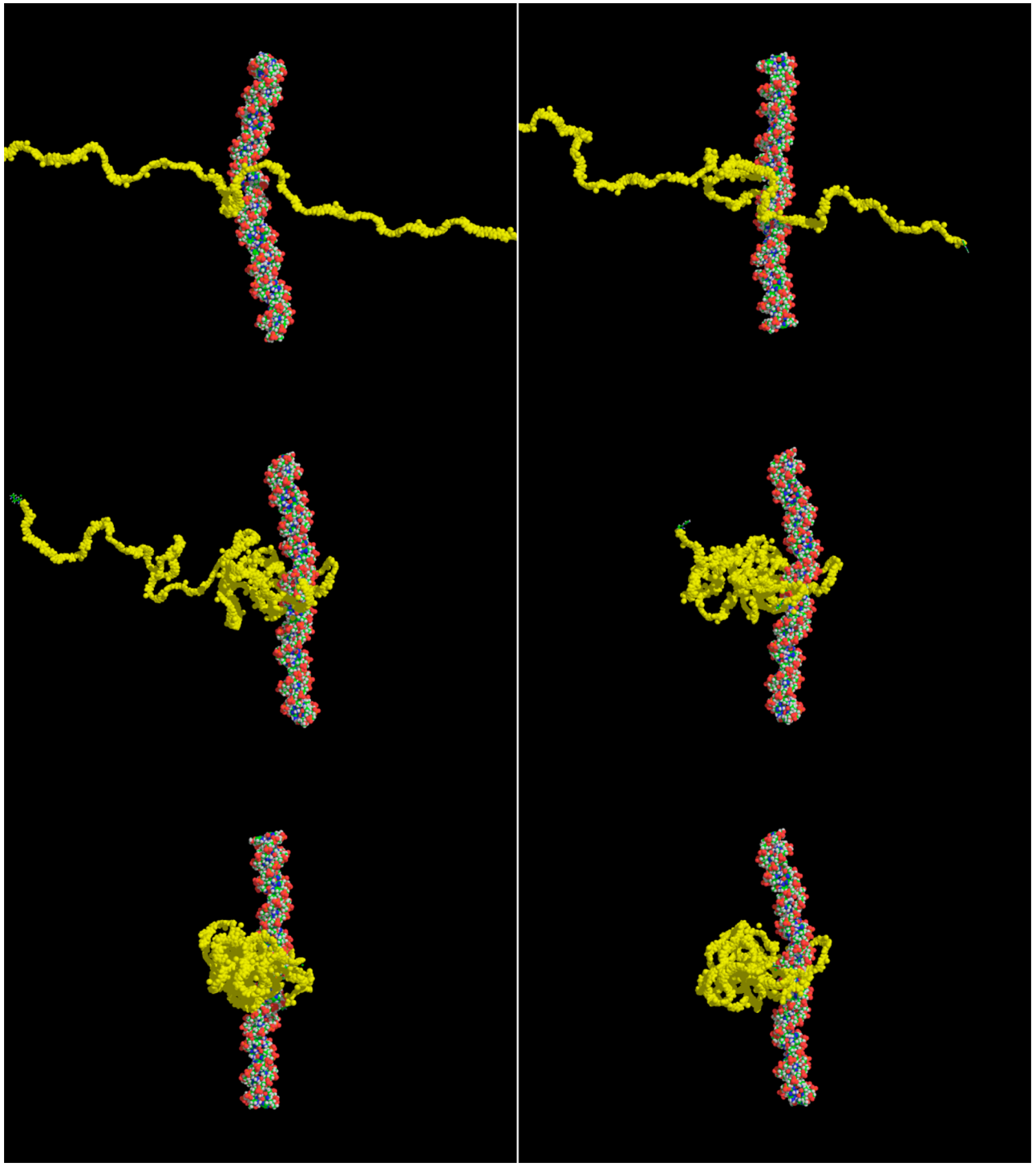

Figure 2. Representative structures selected from a MD simulation of poly$(Py)_{250}$ with a 50-mer DNA duplex after, from top left to bottom right, 28, 36, 54, 66, 80, and 100 ps. No notable change in structure was evident between 100 ps (bottom right image) and the end of the simulation (1000 ps).

which shows the evolution of the final nanowire structure. This comprises a DNA core with CP strands aligned, to some extent, along the helix axis. It is useful to consider an approximate composition of nanowires of average size. A simple representation of a 6 nm diameter nanowire as comprising two cylinders, a 2 nm core of duplex DNA, and the remaining outer shell CP gives, based on molecular volumes, a nanowire with ∼120 polymer strands per DNA duplex. This high CP:DNA strand ratio suggests a relatively small number of DNA···CP interactions compared to CP···CP or CP···solvent interactions. Also, for a typical level of oxidation (one charge per 4 rings)[54] the overall nanowire would bear a high cationic charge as the DNA phosphodiester groups are not sufficient to provide the necessary charge balance. As a result, the association of anions, e.g., chloride, would be expected and are evident in XPS analysis.[41,42] In fact, we find that additional DNA strands can become incorporated into the DNA/CP structure as the nanowire growth process proceeds. This can be

dx.doi.org/10.1021/ja500439v | J. Am. Chem. Soc. 2014, 136, 6649−6655

judged by structure lengths that are longer than individual λ-DNA molecules and by branching, even for Stages 1/2 (see Figures S7−9). This process is in addition to the previously discussed "nanorope" formation[39] which also provides the means by which extended length structures form.

Multiscale Modeling of Polymer Nanowire Formation. As depicted in Scheme 1 we propose the following general mechanism for the formation of smooth, highly regular DNA-templated nanowires. In the first stage of the reaction (Stage 1), oxidation of the monomer forms cationic CP chains, some of which bind to DNA template molecules through supramolecular interactions (electrostatics, hydrogen bonding, van der Waals forces). The formation of such interactions is supported by FTIR spectroscopy, as discussed previously.[42] Initially, the CP chains adopt highly folded, globular, structures which are observed as essentially spherical particles along an individual DNA duplex. These globular structures gradually spread along the helical axis and eventually merge to produce smooth nanowires (Stages 3 → 4). We have investigated the formation of the initial nuclei (Stage 1) using molecular dynamics (MD) simulations. However, the time-scale, hours, for the transformations from Stages 2 → 3 → 4 (Scheme 1) is far too long for atomistic simulation. The latter stages are modeled using a coarse-grained approach[55] described below.

Molecular Dynamics. Figure 2 shows snapshots from a 1000 ps simulation containing a 50-mer DNA duplex and a $(polyPy)_{250}$ strand. This illustrates the formation of a globular particle of the latter bound to the template DNA. Similar results were observed for starting geometries involving either essentially parallel or orthogonal alignment of the two types of polymers. In the early part of the trajectory, after initial interaction between the two polymer strands, the formation of the globular CP particle is promoted by rotation of the DNA about its axis. The structures in Stages 1 and 2 clearly contain CP that has neither maximized the available supramolecular interactions with the template and/or other CP strands nor attained a preferred conformation. The resulting structures are kinetic products of the initial, random, binding.

As the reaction proceeds, and evident from the AFM data, more CP strands bind, increasing the density of particles along the template molecule (Stage 2). Also, there is an increase in particle size, from deposition of more polymer chains and/or further polymerization. The transition Stage 1→ 2 cannot be captured by our coarse-grained model because the linear thermodynamics only applies close to equilibrium and the process depends on details of the nucleation steps and atomic-scale interactions.

Coarse-Grained Model. The maximum reaction times which can be simulated by MD are of the order of ns and therefore can provide information on the early nucleation events (Stage 1), but the growth of the nanowires and the changes in their morphology (2 → 3 → 4) which are observed over periods of hours are not accessible to atomistic simulations. Instead, we have developed a coarse-grained thermodynamic model which treats the growth process in a manner similar to a morphological wetting transition.[56] The changes in morphology are assumed to be governed by similar forces to the wetting of fibers, i.e., the surface tension of the templated material and the free energy of adhesion of CP to the DNA template.[55,57,58] Under the assumption of linear thermodynamics and radial symmetry this leads to an evolution equation for the thickness (h) of the templated material of the form:

$$\mu h\frac{\partial^2 h}{\partial x^2} + \mu\left(\frac{\partial h}{\partial x}\right)^2 = \frac{\partial h}{\partial t} \quad (1)$$

For inorganic materials the terms on the left-hand side can be taken to represent desorption of material and reprecipitation, i.e., an Ostwald-ripening type of process. The second term is always positive and would correspond to precipitation of material, but the first term might correspond to either precipitation or desorption depending on the local curvature. For polymeric materials, as here, the molecular interpretation of these terms is different, involving redistribution of material through dynamic conformation change, but not surface diffusion along the template which would give rise to a fourth order derivative.[59]

Solving eq 1 generates thickness profiles for a nanowire as a function of simulation time. Figure 1d shows the output of a simulation in which the initial condition is a series of particles decorating the template in the manner of Stage 2 (Figure 1a,b,c, column 2). The model reproduces qualitatively our key AFM observations for poly(TPT) and poly(Py) (see SI). The width of the distributions becomes smaller as the system undergoes the transition from Stage 2 → 3 → 4 and the mean height of the structures decreases from Stage 3 → 4. Chemically this is due to the slow spreading of the polymer along the template. Mathematically, it is a consequence of the nonlinear first term in the model (eq 1). In the absence of the factor h, the first term would be conservative, but our previous work[55] shows that redistribution of material from regions which correspond to negative curvature is promoted because they are typically at maxima. Equally, redistribution of materials to regions of positive curvature, is disfavored in the first term because they typically correspond to minima. Finally, we should note that our model cannot reproduce all of the features observed in the data: we cannot describe addition of new material to the template without considering the details of the initial nucleation events. It is also clear that in some AFM images nanowires in different stages are seen. A theoretical description of this requires a stochastic rather than a deterministic model and must include a distribution of nucleation times. Nevertheless, the coarse-grained model presented has the advantage of simplicity and makes two practical predictions useful for the successful formation of smooth nanowires: (i) the process will work best for materials of low surface energy, i.e., regular, smooth nanowires will be easier to prepare for CP than metals ($\gamma \approx 1000$ mN m^{-1} for copper[60] versus $\gamma \approx 30-50$ mN m^{-1} for typical organic polymers[61]) and (ii) the transformation to smooth nanowires is slow because eq 1 has a form similar to a diffusion equation and at long times h varies with $t^{-1/2}$ rather than exponentially as for simple chemical reactions.

■ CONCLUSIONS

These studies reveal details of the mechanism of formation of conductive supramolecular nanowires using DNA-templating. The key factor that enables these conducting polymers to produce the regular nanowire structure is the ability to reorganize on the template once bound. The thermodynamic driving forces are (i) maximization of the available supramolecular interactions (DNA···CP and CP···CP) and (ii) reduction of the surface energy leading to the smooth regular structure of the final nanowire. This is possible due to the reversible nature of the supramolecular interactions. The regularity of these polymeric DNA-templated nanowires is in marked contrast to those formed by other materials, particularly

dx.doi.org/10.1021/ja500439v | J. Am. Chem. Soc. 2014, 136, 6649−6655

metals,[62] which usually show highly granular and sometimes dendritic morphologies. This smooth uniform covering of the template with little apparent defects was also evident from the electrical conductivity along the nanostructures.[38,41,42] Finally, the successful formation of smooth nanowires is the result of a slow reorganization of material on the template and sufficient time must be allowed, typically much greater than the time for the polymerization reaction.

■ ASSOCIATED CONTENT

Supporting Information

Experimental details of sample preparations and characterization, details of the simulation model for producing histograms, theoretical details of the thermodynamic model for templated nanowire growth, AFM data for control experiments showing results of reactions in the absence of DNA, and AFM data showing further examples of DNA/polymer nanowire growth. This material is available free of charge via the Internet at http://pubs.acs.org.

■ AUTHOR INFORMATION

Corresponding Author

andrew.houlton@ncl.ac.uk

Notes

The authors declare no competing financial interest.

■ ACKNOWLEDGMENTS

EU-FP7 LAMAND (Contract no. 245565) and EU ITN NANOEMBRACE (Contract no. 316751).

■ REFERENCES

(1) Lu, W.; Lieber, C. M. *Nat. Mater.* **2007**, *6*, 841.
(2) Huang, Y.; Duan, X.; Wei, Q.; Lieber, C. M. *Science* **2001**, *291*, 630.
(3) Agarwal, R.; Ladavac, K.; Roichman, Y.; Yu, G.; Lieber, C. M.; Grier, D. G. *Opt. Expr.* **2005**, *13*, 8906.
(4) Yu, G.; Lieber, C. M. *Pure Appl. Chem.* **2010**, *82*, 2295.
(5) Braun, E.; Keren, K. *Adv. Phys.* **2004**, *53*, 441.
(6) Seeman, N. C. *Annu. Rev. Biochem.* **2010**, *79*, 65.
(7) Houlton, A.; Watson, S. M. D. *Annu. Rep. Prog. Chem. A* **2011**, *107*, 21.
(8) Service, R. F. *Science* **2011**, *332*, 1140.
(9) Becerril, H. A.; Woolley, A. T. *Chem. Soc. Rev.* **2009**, *38*, 329.
(10) Winfree, E. *Nature* **1998**, *394*, 539.
(11) Dietz, H.; Douglas, S. M.; Shih, W. M. *Science* **2009**, *325*, 725.
(12) Seeman, N. C. *Nature* **2003**, *421*, 427.
(13) Rothemund, P. W. K. *Nature* **2006**, *440*, 297.
(14) Li, H.; Carter, J. D.; LaBean, T. H. *Mater. Today* **2009**, *12*, 24.
(15) Nangreave, J.; Han, D.; Liu, Y.; Yan, H. *Curr. Opin. Chem. Biol.* **2010**, *14*, 608.
(16) Ke, Y. G.; Ong, L. L.; Shih, W. M.; Yin, P. *Science* **2012**, *338*, 1177.
(17) Keren, K.; Berman, R. S.; Buchstab, E.; Sivan, U.; Braun, E. *Science* **2003**, *302*, 1380.
(18) Mirkin, C. A. *Inorg. Chem.* **2000**, *39*, 2258.
(19) Macfarlane, R. J.; O'Brien, M. N.; Petrosko, S. H.; Mirkin, C. A. *Angew. Chem., Int. Ed.* **2013**, *52*, 5688.
(20) Kim, Y.; Macfarlane, R. J.; Mirkin, C. A. *J. Am. Chem. Soc.* **2013**, *135*, 10342.
(21) Macfarlane, R. J.; Jones, M. R.; Lee, B.; Auyeung, E.; Mirkin, C. A. *Science* **2013**, *341*, 1222.
(22) Braun, E.; Eichen, Y.; Sivan, U.; Ben-Yoseph, G. *Nature* **1998**, *391*, 775.
(23) Becerril, H. A.; Stolenberg, R. M.; Wheeler, D. R.; Davis, R. C.; Harb, J. N.; Woolley, A. T. *J. Am. Chem. Soc.* **2005**, *127*, 2828.
(24) Al-Hinai, M. N.; Hassanien, R.; Wright, N. G.; Horsfall, A. B.; Houlton, A.; Horrocks, B. R. *Faraday Discuss.* **2013**, *164*, 71.
(25) Al-Said, S. A. F.; Hassanien, R.; Hannant, J.; Galindo, M. A.; Pruneanu, S.; Pike, A. R.; Houlton, A.; Horrocks, B. R. *Electrochem. Commun.* **2009**, *11*, 550.
(26) Watson, S. M. D.; Wright, N. G.; Horrocks, B. R.; Houlton, A. *Langmuir* **2010**, *26*, 2068.
(27) Houlton, A.; Pike, A. R.; Galindo, M. A.; Horrocks, B. R. *Chem. Commun.* **2009**, 1797.
(28) Yan, H.; Park, S. H.; Finkelstein, G.; Reif, J. H.; LaBean, T. H. *Science* **2003**, *301*, 1882.
(29) Deng, Z.; Mao, C. *Nano Lett.* **2003**, *3*, 1545.
(30) Park, S. H.; Barish, R.; Li, H. Y.; Reif, J. H.; Finkelstein, G.; Yan, H.; LaBean, T. H. *Nano Lett.* **2005**, *5*, 693.
(31) Becerril, H. A.; Stoltenberg, R. M.; Wheeler, D. R.; Davis, R. C.; Harb, J. N.; Woolley, A. T. *J. Am. Chem. Soc.* **2005**, *127*, 2828.
(32) Geng, Y. L.; Liu, J. F.; Pound, E.; Gyawali, S.; Harb, J. N.; Woolley, A. T. *J. Mater. Chem.* **2011**, *21*, 12126.
(33) Liu, J. F.; Geng, Y. L.; Pound, E.; Gyawali, S.; Ashton, J. R.; Hickey, J.; Woolley, A. T.; Harb, J. N. *ACS Nano* **2011**, *5*, 2240.
(34) Geng, Y. L.; Pearson, A. C.; Gates, E. P.; Uprety, B.; Davis, R. C.; Harb, J. N.; Woolley, A. T. *Langmuir* **2013**, *29*, 3482.
(35) Nagarajan, R.; Liu, W.; Kumar, J.; Tripathy, S. K.; Bruno, F. F.; Samuelson, L. A. *Macromolecules* **2001**, *34*, 3921.
(36) Ma, Y.; Zhang, J.; Zhang, G.; He, H. *J. Am. Chem. Soc.* **2004**, *126*, 7097.
(37) Nickels, P.; Dittmer, W. U.; Beyer, S.; Kotthaus, J. P.; Simmel, F. C. *Nanotechnology* **2004**, *15*, 1524.
(38) Dong, L.; Hollis, T.; Fishwick, S.; Connolly, B. A.; Wright, N. G.; Horrocks, B. R.; Houlton, A. *Chem.—Eur. J.* **2007**, *13*, 822.
(39) Pruneanu, S.; Al-Said, S. A. F.; Dong, L.; Hollis, T. A.; Galindo, M. A.; Wright, N. G.; Houlton, A.; Horrocks, B. R. *Adv. Funct. Mater.* **2008**, *18*, 2444.
(40) Hannant, J.; Hedley, J. H.; Pate, J.; Walli, A.; Farha Al-Said, S. A.; Galindo, M. A.; Connolly, B. A.; Horrocks, B. R.; Houlton, A.; Pike, A. R. *Chem. Commun.* **2010**, *46*, 5870.
(41) Hassanien, R.; Al-Hinai, M.; Farha Al-Said, S. A.; Little, R.; Siller, L.; Wright, N. G.; Houlton, A.; Horrocks, B. R. *ACS Nano* **2010**, *4*, 2149.
(42) Watson, S. M. D.; Hedley, J. H.; Galindo, M. A.; Al-Said, S. A. F.; Wright, N. G.; Connolly, B. A.; Horrocks, B. R.; Houlton, A. *Chem.—Eur. J.* **2012**, *18*, 12008.
(43) Ikeda, M.; Nobori, T.; Schmutz, M.; Lehn, J. M. *Chem.—Eur. J.* **2005**, *11*, 662.
(44) Sreenivasachary, N.; Hickman, D. T.; Sarazin, D.; Lehn, J. M. *Chem.—Eur. J.* **2006**, *12*, 8581.
(45) Ustinov, A.; Weissman, H.; Shirman, E.; Pinkas, I.; Zuo, X.; Rybtchinski, B. *J. Am. Chem. Soc.* **2011**, *133*, 16201.
(46) Llanes-Pallas, A.; Yoosaf, K.; Traboulsi, H.; Mohanraj, J.; Seldrum, T.; Dumont, J.; Minoia, A.; Lazzaroni, R.; Armaroli, N.; Bonifazi, D. *J. Am. Chem. Soc.* **2011**, *133*, 15412.
(47) The elegant work of Schuster et al. offers an alternative route to materials comprising DNA and organic groups suitable for forming CP, such as TPT and aniline (refs 48−50). This approach is quite different however, as it is involves strong covalent bonding between the CP and the DNA rather than supramolecular interactions, as here.
(48) Chen, W.; Guler, G.; Kuruvilla, E.; Schuster, G. B. *Macromolecules* **2010**, *43*, 4032.
(49) Chen, W.; Josowicz, M.; Datta, B.; Schuster, G. B.; Janata, J. *Electrochem. Solid State Lett.* **2008**, *11*, E11.
(50) Chen, W.; Schuster, G. B. *J. Am. Chem. Soc.* **2013**, *135*, 4438.
(51) Richter, J.; Seidel, R.; Kirsch, R.; Mertig, M.; Pompe, W.; Plaschke, J.; Schackert, H. K. *Adv. Mater.* **2000**, *12*, 507.
(52) Blackburn, G. M.; Gait, M. J. *Nucleic Acids in Chemistry and Biology*; 2nd ed.; OUP: Oxford, 1997.
(53) While AFM tip convolution effects may prevent sufficiently small breaks in the coatings from being resolved, support for the claim, that the CP nanowires are continuous, is provided by their demonstrated electrically conducting nature.

(54) Bredas, J. L.; Street, G. B. *Acc. Chem. Res.* **1985**, *18*, 309.
(55) Watson, S. M. D.; Houlton, A.; Horrocks, B. R. *Nanotechnology* **2012**, *23*, 505603.
(56) Lipowsky, R. *Curr. Opin. Colloid Interface Sci.* **2001**, *6*, 40.
(57) Brochard, F. *J. Chem. Phys.* **1986**, *84*, 4664.
(58) Lukas, D.; Pan, N. *Polym. Compos.* **2003**, *24*, 314.
(59) Wolf, D. E.; Villain, J. *Europhys. Lett.* **1990**, *13*, 389.
(60) Udin, H.; Shaler, A. J.; Wulff, J. *Trans. AIME* **1949**, *185*, 186.
(61) http://www.accudynetest.com/polytable; Diversified Enterprises: Claremont, NH; Downloaded January, 2014.
(62) Richter, J.; Mertig, M.; Pompe, W.; Monch, I.; Schackert, H. K. *Appl. Phys. Lett.* **2001**, *78*, 536.